ChemComm

Accepted Manuscript

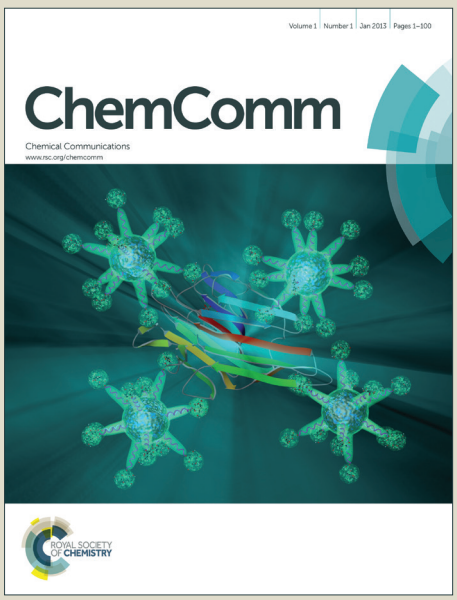

ROYAL SOCIETY OF CHEMISTRY

www.rsc.org/chemcomm

Cite this: DOI: 10.1039/c0xx00000x

www.rsc.org/xxxxxx

ARTICLE TYPE

Self-assembled ultrathin crystalline polymer film for high performance phototransistors

Hui Li,[a,b] Yishi Wu,[a] Xuedong Wang,[a,b] Qinghua Kong [a,b] and Hongbing Fu*[a,c]

Received (in XXX, XXX) Xth XXXXXXXXX 20XX, Accepted Xth XXXXXXXXX 20XX

DOI: 10.1039/b000000x

Π-conjugated polymer, PQBOC8, can be easily assembled into large-area crystalline ultrathin film at $CHCl_3$/water interface. Phototransistor based on this ultrathin film showed a large photoresponsivity of 970 A W^{-1}, and a photocurrent/dark current ratio of 1.36×10^4 under very low white light irradiation.

Polymer semiconductors have been widely recognized as promising materials for large-area, flexible electronic devices due to film forming capacity and mechanical flexibility.[1-3] However, many limitations in the performance of current polymer electronics, including organic field effect transistor (OFET) and solar cell, are attributed to lack of macroscopic order in polymer films and inability to control the morphology at nanoscale level.[4] In contrast to devices based on organic amorphous thin films, organic single crystals possess higher molecular ordering which hold a promise for enhanced performance and even unique optical and electronic properties.[5, 6] However, in consideration of conformational freedom of alkyl and flexible entanglement of backbone, polymers tend to form disordered structure at nanometer to micrometer length scale.[7, 8] Therefore, it is a challenge to fabricate polymer into crystalline nanostructures.

Solution-phase self-assembly has been demonstrated for an efficient method to prepare crystalline polymer with one-dimensional (1D) nanostructure.[9-11] For example, Xia and co-workers reported the charge transport of 1D nanobelts from n-type polymer BBL fabricated by solution phase synthesis.[10] Zhan et al. prepared highly crystalline PTz nanowires with excellent phototransistor performance by evaporation of dilute solution.[12] Compared with 1D nanostructure, two-dimensional (2D) crystalline materials, like graphene, attract much attention owing to their molecular-scale thickness with huge surface areas and compatibility with arbitrary substrates.[13] They are endowed great expectation for next generation electronics.[14-16] To obtain 2D highly ordered nanostructures, in previous studies, copolymers were designed to have a plethora of molecular interaction, including hydrogen bonding, electrostatic, dipole-dipole, amphiphilic blocks, etc.[17, 18] Tremendous efforts have to been focused on the design and synthesis to meet these requirements. What's more, this is not suitable for polymers with given structures. Therefore, the establishment of a facile approach to fabricate π-conjugated polymer into 2D crystalline film is of great practical value not only in terms of the relationship between its intrinsic structure and properties, but also for technical application. To our knowledge, large-area and ultrathin polymer films with high crystallinity via solution-phase self-assembly has not been achieved.

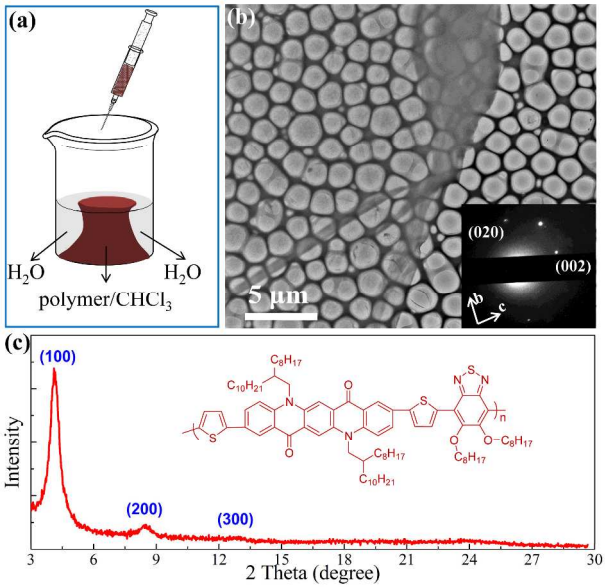

Fig.1 (a) Schematic illustration for the preparation of 2D film. (b) A TEM image of **PQBOC8** 2D film. The inset shows a selected area electron diffraction (SAED) pattern for this corresponding film. (c) XRD pattern of 2D film on SiO_2/Si substrate. The inset is the molecular structure of polymer **PQBOC8**.

Herein, we reported a simple self-assemble process for organizing free-stretched polymer chains into ordered 2D crystalline ultrathin film in a large scale at $CHCl_3$/water interface. We choose polymer **PQBOC8** as sample which is a promising semiconductor used in optoelectronic devices for its high charge-carrier mobility[19] and power conversion efficiency in solar cell,[20] simultaneously. The polymer was synthesized by Suzuki coupling according to previous reported procedure.[19] Wide absorption range (see in ESI†) and the high fluorescence quantum yield of 10% in solid state may endow it good candidate of photo-controlled devices.

Fig. 1a shows the schematic representation of the preparation method of **PQBOC8** nanostructure. Firstly, 1 mL deionized water was put into a beaker. Polymer **PQBOC8** was totally soluble in $CHCl_3$ and then dropwisely injected into the container. Finally, a cover was put on the beaker to guarantee the slow evaporation of

$CHCl_3$ and give the polymer molecules sufficient time to adjust themselves. Because of larger density of $CHCl_3$ over water, $CHCl_3$ embedded into water and retained part of solution touching air for evaporation. After complete evaporation of $CHCl_3$, the 2D films floated on the water surface. It is worthy to note that we extended this method to other typical polymers including P3HT and PBDTTT-C-T (Fig. S2). These polymers could also be assembled into large-area films indicating this method broadly applicable.

The morphology of 2D **PQBOC8** films was characterized by transmission electron microscopy (TEM) as shown in Fig. 1b. The size of the film is about hundreds of micrometers. The electron diffraction pattern (inset of Fig. 1b) indicates that this film is highly crystalline. Electron beam damage is particularly problematic for ultrathin polymers film. With this in mind, the electron diffraction image was taken at 208 K. Indexation is assigned in a similar way as for P3HT.[21, 22] We ascribe a *d*-spacing of 4.0 Å from (020) reflection along b axis to π-π stacking distance and 4.4 Å from (002) reflection along c axis to the reflection of polymer chain direction. To acquire a better understanding of molecular packing in crystalline film, X-ray diffraction (XRD) measurement was employed and shown in Fig. 1c. Strong and sharp diffraction peak is observed at $2\theta = 4.1^{\circ}$ while the second and third diffraction peaks are also observed at $2\theta = 8.3^{\circ}$, and $2\theta = 12.3^{\circ}$, which arise from ordered lamellar structure with a interlayer *d*-spacing of 21.5 Å. In combination with the result of electron diffraction pattern, we could confirm that only edge-on configuration existed in the crystalline films. This is different from the result of the spin-coated film in which edge-on and face-on orientation were concomitant.[19] That is to say, the molecules packed much ordered in films prepared by this novel method.

High resolution TEM (HR-TEM) was used to visualize the inner morphology of thin film. As shown in Fig. 2a, the polymer backbones show long-range orientational order even though there are fluctuations in the degree of local order. Over larger length scales, film morphology was observed by atomic force microscopy (AFM). In Fig. 2b, strip-shaped structures were observed and intertwined together forming large-area film. In order to obtain the intermediate state of the solution, we observed the morphology of sample by TEM before all $CHCl_3$ evaporation. Dispersing nanobelts were numerously existent (Fig. S3a) before all $CHCl_3$ was evaporated which shed more light on the formation large-area film. The thickness and morphology of these films can be controlled by adjusting the concentration of the initial solution (Fig. S4). The self-assembled films have a range of thickness from 22 nm to 14 nm with the decrease of concentration of solution (Table S1). When the solution concentration of **PQBOC8** was given at 0.1 mg mL^{-1}, the nuclear density was so high that they easily formed network and disordered structures. With the concentration of the solution decreasing, the density of nuclear would also decrease and the film becomes much ordered. For instance, it is obvious that film with aligned nanostructure can be obtained at the concentration of 0.005 mg mL^{-1}. Nonetheless, the film would become discontinuous when the concentration below 0.005 mg mL^{-1}.

On the basis of above observation and discussion, we proposed a possible mechanism in Fig. 3 for formation of 2D crystalline film. At first step, the polymer chains are fully extended in diluted solution (Fig. 3a). With the evaporation of $CHCl_3$, molecules can attach each other through electrostatic interaction and π-π interaction of donor and acceptor units between adjacent chains forming local ordered strips as nucleation (Fig. 3b). As more $CHCl_3$ evaporated, the $CHCl_3$/water interface would continuously shrink to reduce the surface energy which induced a force to compress the strips to arrange in a more ordered manner (Fig. 3c). With the help of surface tension of water, the shrinking occurs along all direction of interface, and thus leads to the formation of large-area 2D films with polymer side chains perpendicular to the substrate (Fig. 3d).

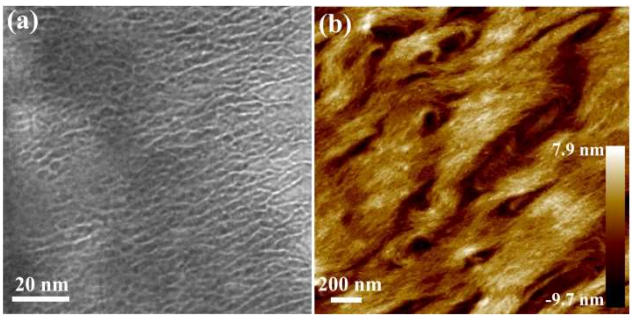

Fig.2 (a) HR-TEM of 2D ultrathin film. (b) Height image of 2D ultrathin film on a silicon wafer at concentration of 0.005 mg mL^{-1}.

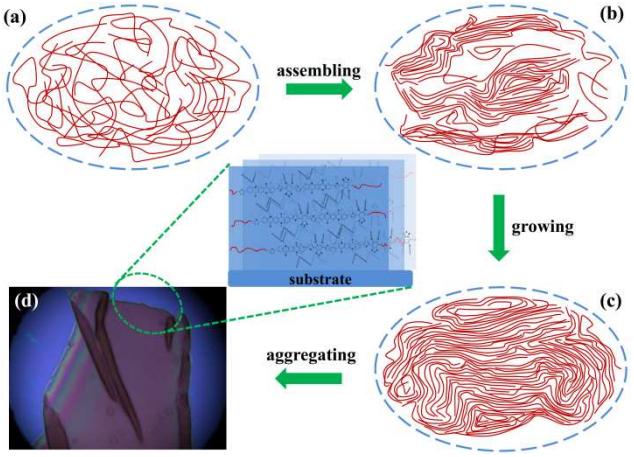

Fig.3 Schematic illustration of 2D crystalline film self-assemble process at $CHCl_3$/water interface and a bright-field optical microscopy image of the 2D crystalline film.

In order to examine the electrical properties of crystalline films, OFET devices with top-contact and bottom-gate configuration were fabricated. The relationship of thickness and mobilities are shown in Table S1. The mobility increases with the thickness of the film decreasing, which is in accordance with the fact that the film becomes much ordered with the thickness decreasing. The maximum mobility was found to be 0.13 $cm^2 V^{-1} s^{-1}$ with on/off current ratio of 10^7 at the concentration of 0.005 mg mL^{-1} while the devices were determined without any post-treatments. The typical output and transfer characteristics are shown in Fig. S6. The mobility will be improved if the substrate was treated with proper monolayer dielectric and some wrinkles could be eliminated in the process of transferring from water. Further investigation is still ongoing.

Typical photoresponse characteristics of phototransistors are shown in Fig. 4a and 4b. The increase of drain current was

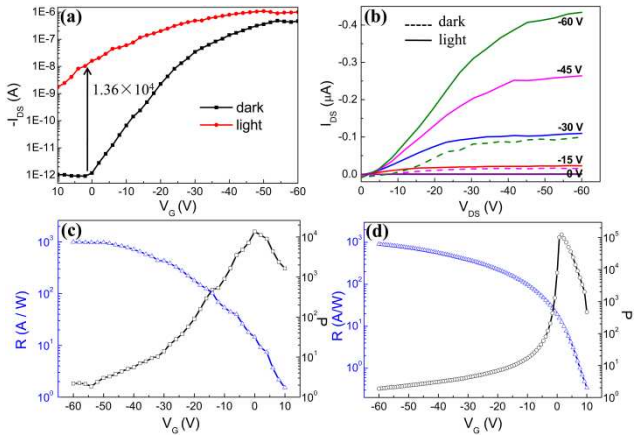

Fig.4 (a) Transfer and (b) output characteristics based on 2D crystalline polymer film transistor in the dark and under white light irradiation with an optical power density of 0.28 mW cm^{-2}. (c) Photoresponsivity and photocurrent/dark current ratio under white light power intensity of 0.28 mW cm^{-2} and (d) under green light power intensity of 43 μW cm^{-2} with varied V_{GS} at V_{DS} = -60 V.

obviously observed under the illumination, which indicates that light plays an important role to improve the performance of the transistor. This conclusion is further confirmed by the results of Fig. S7. That is to say, light irradiation can be as a substitute of V_G to adjust the drain current and control the on/off state of the devices.[23] Photoresponsivity (R) and photocurrent/dark current ratio (P) are defined by the equations given in supporting information. As shown in Fig. 4c, under a low white light irradiation of 0.28 mW cm^{-2}, the phototransistor device exhibits strong photo-dependence and high light sensitivity with a R value of 970 A/W and a P value of 1.36×10^4. The phototransistor performance is also analyzed on irradiation at different wavelengths (Fig. S8 and Table S2). Green light irradiation yields the largest enhancement in the drain current with photoresponsivity of 1000 A W^{-1} and maximum on/off ratio of 1.24×10^5 under very low power intensity of 43 μW cm^{-2} (Fig. 4d). This is attributed to the wavelength of the light source matches the light absorption range. The photoresponsivity reported here is among the highest values for devices based on the conjugated polymers. The phototransistor based on the spin-coated film only shows the highest R of 106 A W^{-1} and P of 92 under the same experiment condition (Fig. S9). We propose possible reasons for the highly sensitive phenomenon of the crystalline film and its superiority than the spin-coated film in view of intrinsic properties of **PQBOC8**. Firstly, that the solid fluorescence quantum yield (Φ) of 10% is larger than many other donor-acceptor type polymers determines the exciton quality and numbers. Secondly, slowly self-assembly induces highly ordered crystalline structure leading to a decrease in defects as trapping sites. Moreover, donor units and acceptor units in adjacent polymer chains pack with each other much closely. This leads to faster charge transfer in crystalline film than that of spin-coated film, in which donor units and acceptor units are arbitrary. This speculation can be confirmed by time-resolved fluorescence measurements (Fig. S10). The emission of both the samples follows a two-exponential decay. We ascribe the long-lived component to the charge transfer (CT) between the donor and acceptor moieties within one polymer chain while the short-lived component arises from CT between the donor and acceptor units in adjacent polymer chains.[24] The ratio of the fast component in the crystalline film is higher than that in amorphous film (72% vs. 45%), indicating that directional inter-chain charge transfer interaction play a dominant role in the depopulation of the excited state. It would lead to efficient exciton dissociation and increased photoresponsivity in the phototransistor device based on self-assembled polymer film.

In summary, we successfully prepared large-area crystalline polymer film by a simple $CHCl_3$/water interface method. In the crystalline film, polymers constitute edge-on orientation which is much ordered than the film prepared via spin-coating method. Phototransistors based on these ultrathin films exhibited high R value of 970A W^{-1} and on/off ratio up to 1.36×10^4 under low white light irradiation. This methodology provides a general and efficient strategy to prepare crystalline polymer films which have great potential to be applied in optoelectronics.

This work was supported by the National Natural Science Foundation of China (Nos. 21073200, 21273251, 91333111, 21190034, 21221002), Beijing Municipal Science & Technology Commission (No. Z131103002813097), project of Construction of Innovative Teams and Teacher Career Development for Universities and Colleges Under Beijing Municipality (IDHT20140512), the National Basic Research Program of China (973) 2011CB808402, 2013CB933500, and the Chinese Academy of Sciences.

Notes and references

[a] *Beijing National Laboratory for Molecular Science (BNLMS), Institute of Chemistry, Chinese Academy of Science, Beijing 100190, P. P. China. Fax: +86-10-62526801; Tel: +86-10-62526801; E-mail: hongbing.fu@iccas.ac.cn.*
[b] *Graduate University of Chinese Academy of Sciences (GUCAS), Beijing 100049, P. R. China.*
[c] *Beijing Key Laboratory for Optical Materials and Photonic Devices, Department of Chemistry, Capital Normal University, Beijing 100048, P. R. China.*

† Electronic Supplementary Information (ESI) available: Experimental details, fabrication procedures, UV/vis and photoluminescence spectra, bright-field optical microscopy images, TEM and AFM images, OFET and phototransistor performances, and fluorescence lifetime measurerment . See DOI: 10.1039/b000000x/

1 Y. J. Cheng, S. H. Yang and C. S. Hsu, *Chem. Rev.*, 2009, **109**, 5868-5923.
2 P. M. Beaujuge and J. M. Frechet, *J. Am. Chem. Soc.*, 2011, **133**, 20009-20029.
3 P. Bujak, I. Kulszewicz-Bajer, M. Zagorska, V. Maurel, I. Wielgus and A. Pron, *Chem. Soc. Rev.*, 2013, **42**, 8895-8999.
4 T. Lei, J.-H. Dou and J. Pei, *Adv. Mater.*, 2012, **48**, 6457-6461.
5 F. S. Kim, G. Ren and S. A. Jenekhe, *Chem. Mater.*, 2010, **23**, 682-732.
6 X. Wang, Q. Liao, Q. Kong, Y. Zhang, Z. Xu, X. Lu and H. Fu, *Ang. Chem. Int. Ed.*, 2014, **126**, 5973-5977.
7 M. Brinkmann and J. C. Wittmann, *Adv. Mater.*, 2006, **18**, 860-863.
8 Y. Liu, H. Wang, H. Dong, L. Jiang, W. Hu and X. Zhan, *Small*, 2012, 294-299.
9 S. Berson, R. De Bettignies, S. Bailly and S. Guillerez, *Adv. Funct. Mater.*, 2007, **17**, 1377-1384.
10 A. L. Briseno, S. C. B. Mannsfeld, P. J. Shamberger, F. S. Ohuchi, Z. Bao, S. A. Jenekhe and Y. Xia, *Chem. Mater.*, 2008, **20**, 4712-4719.
11 H. Dong, S. Jiang, L. Jiang, Y. Liu, H. Li, W. Hu, E. Wang, S. Yan, Z. Wei, W. Xu and X. Gong, *J. Am. Chem. Soc.*, 2009, **131**, 17315-17320.

12 Y. Liu, H. Dong, S. Jiang, G. Zhao, Q. Shi, J. Tan, L. Jiang, W. Hu and X. Zhan, *Chem. Mater.*, 2013, **25**, 2649-2655.
13 L. Jiang, H. Dong, Q. Meng, H. Li, M. He, Z. Wei, Y. He and W. Hu, *Adv. Mater.*, 2011, **23**, 2059-2063.
14 J. C. Meyer, A. K. Geim, M. I. Katsnelson, K. S. Novoselov, T. J. Booth and S. Roth, *Nature*, 2007, **446**, 60-63.
15 M. Osada and T. Sasaki, *Adv. Mater.*, 2012, **24**, 210-228.
16 X. Song, J. Hu and H. Zeng, *J. Mater. Chem. C*, 2013, **1**, 2952-2969.
17 J. del Barrio, L. Oriol, C. Sánchez, J. L. Serrano, A. Di Cicco, P. Keller and M.-H. Li, *J. Am. Chem. Soc.*, 2010, **132**, 3762-3769.
18 Z. Yin and Q. Zheng, *Adv. Energy. Mater.*, 2012, **2**, 179-218.
19 H. Li, C. Gu, L. Jiang, L. Wei, W. Hu and H. Fu, *J. Mater. Chem. C*, 2013, **1**, 2021-2027.
20 H.-J. Song, D.-H. Kim, E.-J. Lee, S.-W. Heo, J.-Y. Lee and D.-K. Moon, *Macromolecules*, 2012, **45**, 7815-7822.
21 M. Brinkmann, E. Gonthier, S. Bogen, K. Tremel, S. Ludwigs, M. Hufnagel and M. Sommer, *ACS Nano*, 2012, **6**, 10319-10326.
22 Z. Yu, H. Yan, K. Lu, Y. Zhang and Z. Wei, *RSC Adv.*, 2012, **2**, 338-343.
23 Y. Liu, H. Wang, H. Dong, J. Tan, W. Hu and X. Zhan, *Macromolecules*, 2012, **45**, 1296-1302.
24 H. Liu, H. Jia, L. Wang, Y. Wu, C. Zhan, H. Fu and J. Yao, *Phys. Chem. Chem. Phys.*, 2012, **14**, 14262-14269.